Electrochimica Acta 247 (2017) 826–834

Contents lists available at ScienceDirect

Electrochimica Acta

journal homepage: www.elsevier.com/locate/electacta

Electrochemical grafting passivation of silicon via electron transfer at polymer/silicon hybrid interface

Jianhui Chen[a], Yanjiao Shen[a], Jianxin Guo[a], Bingbing Chen[a], Jiandong Fan[a,b,*], Feng Li[c], Baoting Liu[a], Haixu Liu[a], Ying Xu[a], Yaohua Mai[a,b,*]

[a] Institute of Photovoltaics, College of Physics Science and Technology, Hebei University, Baoding 071002, China
[b] Institute of New Energy Technology, College of Information and Technology, Jinan University, Guangzhou, 510632, China
[c] State Key Laboratory of Photovoltaic Materials & Technology, Yingli Green Energy Holding Co., Ltd., Baoding 071051, China

ARTICLE INFO

Article history:
Received 2 May 2017
Received in revised form 7 July 2017
Accepted 11 July 2017
Available online 12 July 2017

Keywords:
polymer
surface passivation
lifetime
electrochemical
interface

ABSTRACT

The most important aspect in the development of Si-based photovoltaic technologies is the passivation of the Si wafer surface. Here, we show that Poly(3,4-ethylthiophene):polystyrenesulfonate (PEDOT:PSS) thin films, frequently used in organic/inorganic hybrid solar cells as emitter layers, provide an excellent surface passivation with a millisecond (ms) level effective minority carrier lifetime (τ_{eff}). More importantly, we find that this passivation effect is dominated by the PSS species in PEDOT:PSS rather than PEDOT ones. The PSS thin film passivation yields a high τ_{eff} of 9.4 ms on a high-resistivity Si wafer. The interface nature of PSS/Si is unveiled by the X-ray photoelectron spectroscopy and first-principles total-energy calculations together. An electrochemical passivation mechanism is clarified: the Si sub-oxides form at PSS/Si interface by the electrochemical grafting O groups in PSS onto Si surface, which can be controlled by injecting holes or electrons into the Si surface, leading to a switchable interface state between oxidation and deoxidation. To examine the application of the passivation strategy in real devices, we develop a polymer-passivated both-sides Si heterojunction solar cell with light-induced enhancement of photovoltaic performances, which is consistent with the light-induced enhancement of τ_{eff}.

1. Introduction

The suppression of surface/interface recombination through the application of a thin passivation layer on the silicon (Si) wafer surface is central to research and development efforts in advanced photovoltaic (PV) technologies [1–3]. An excellent passivation scheme can be utilized to enable the measurement of Si material properties and the prediction of solar cell precursor performance [4,5]. In addition, a high level of surface passivation is a basic prerequisite for high-efficiency crystalline Si (c-Si) solar cells [6–9]. Two passivation schemes, namely, chemical passivation or field passivation, have been successfully developed for Si PVs [10,11]. Chemical passivation aims to reduce the interface defects, i.e., unsaturated Si dangling bonds with atomic oxygen or hydrogen in the materials, via a chemical reaction between Si and the passivating materials. The typical passivating materials used are SiO_2 and hydrogenated amorphous silicon (a-Si:H) [12,13]. The field passivation strategy aims to repel minority carriers from the c-Si surface by applying an internal electric field induced by the fixed charge in materials such as SiN_x [14] and Al_2O_3 [2,8]. An advantage of these schemes is the achievement of decent passivation effect, which is typically evaluated by means of the effective minority carrier lifetime (τ_{eff}) [15,16] (Supplementary Fig. S1a). The impressive realization of a millisecond (ms) range of τ_{eff} using Al_2O_3 [2] and a-Si:H [17] passivation gives rise to two types of high-efficiency solar cells in industry, i.e., passivated emitter and rear contact (PERC) solar cells that are passivated by Al_2O_3 on the back surface [18], and heterojunction with intrinsic thin layer (HIT) solar cells that are passivated by a-Si:H on both sides [19,20]. The disadvantages of these schemes include a requirement of a vacuum or high-temperature condition as well as the possible utilization of the explosive gas source, such as silane and trimethylaluminium (TMA).

* Corresponding author at: Institute of Photovoltaics, College of Physics Science and Technology, Hebei University, Baoding 071002, China.
E-mail addresses: chenjh.0403@163.com (J. Chen), jdfan@jnu.edu.cn (J. Fan), yaohuamai@jnu.edu.cn (Y. Mai).

http://dx.doi.org/10.1016/j.electacta.2017.07.071
0013-4686/

By contrast, hybrid solar cells composed of a conductive polymer, poly (3,4-ethylthiophene):polystyrenesulfonate (PEDOT:PSS) (the chemical formulae of the constituents are shown in Supplementary Fig. S1b and c) coated on a Si wafer, have recently garnered much attention because of the following unique advantages compared with conventional Si PV technologies: a low-temperature fabrication process, simple device geometry, and potentially low-cost nature [21–23]. However, the power conversion efficiencies (PCE) of hybrid cells still suffer from lower values (typically below 10%) than that of conventional c-Si solar cells (typically 18-21% in the production line and 26% in the laboratory) [6,20]. One reason for the low efficiency of hybrid solar cells is the lack of a powerful passivation scheme, which leads to either the utilization of the native oxide layer to passivate the Si surface or the absence of any passivation on the surface [24]. Some researchers have also attempted to introduce passivation materials from conventional c-Si solar cells into hybrid cells, such as the aforementioned Al_2O_3 and SiO_2, and an improvement in the cell performance was observed [25–27]. Clearly, overcoming the challenge of surface passivation is essential to the future success of the development of hybrid solar cells.

HF or iodine-methanol, as a simple passivation scheme, has been used for the lifetime measurement of Si wafers in industry, but their applications are limited by the low τ_{eff} and the inconvenient operation that samples need to be dipped in a chemical solution [28,29]. It was also mentioned that PEDOT:PSS itself has a little passivation effect, which was confirmed by several low τ_{eff} values of 49–317 μs [30,31]. To date there are still little works done regarding a high-quality passivation scheme with mild fabrication conditions (less-hazardous, vacuum-free, low temperature and easy-to-use operation).

In this work, very high lifetimes (4–9 ms) are obtained for high-resistivity silicon wafers passivated by PEDOT:PSS or even PSS alone. This high quality passivation, on the one hand, is linked to one key finding that the major contributor to passivation is from the PSS species in the PEDOT:PSS blend material system rather than from the PEDOT species. On the other hand, we demonstrated that unlike the traditional passivation mechanism, via a chemical reaction or a field-effect, the passivation of Si surface by PSS stems from an electrochemical oxidation at the PSS/Si interface, which can be controlled by electron transfer at the Si surface. We tuned the electron transfer by light soaking, applied potential and atmosphere, leading to the light, potential and oxygen-induced enhancement effect of τ_{eff}.

The immediate question that arises is why this high-quality passivation effect has eluded researchers thus far. First, because the major contributor to passivation is the PSS, high-quality passivation should be obtained from PEDOT:PSS with a high percentage of PSS species. For example, in this paper, the following three types of PEDOT:PSS materials are introduced: PH1000 (the ratios of PEDOT to PSS is 1:2.5), AI4083(1:6) and CH8000(1:20) (all from Clevios). However, in the fabrication of hybrid solar cells, it is well known that suitable additives, e.g., dimethyl sulfoxide (DMSO), N,N-dimethylformamide (DMF), and ethylene glycol, must be added to PH1000 or AI4083 to increase the material's conductivity as an effective emitter or window layer [32,33]. But it has been reported that the addition of DMSO can decrease the percentage of PSS [34,35]. This step would unintentionally destroy the passivation effect. Second, the passivation strategy of PSS is an electrochemical grafting that generated sub-oxides at the PSS/Si interface by a redox reaction. In this case, passivation need to be activated by external excitation, such as light soaking and applied potential (the methods used in this work).

This passivation scheme is examined in a solar cell application based on understanding of the passivation origin. To solve the discrepancy between the passivation effect and the conductivity of PEDOT:PSS, we develop a polymer-passivated both-sides Si heterojunction solar cell by incorporating PEDOT:PSS layers with a proper percentage of PSS into both interfaces. It is observed that the open circuit voltage (V_{oc}) of the device increase as the light soaking time increases, which is consistent with the light-induced enhancement of τ_{eff}.

2. Experimental

2.1. Thin film fabrication

Si wafers, 370 μm-thick n-type (100)-oriented float zone (3–5 kΩ·cm), with double side polished surfaces were used as the substrate materials to evaluate passivation. The size of the wafers is 2 inches to enable the lifetime measurement by a Sinton tool. Si wafers were first dipped into hydrofluoric acid (HF) to remove the native oxide layer, which resulted in a H-terminated Si surface with Si-H bonds and dangling bond defects (Supplementary Fig. S1d). Subsequently, three types of PEDOT:PSS (PH1000, AI4083 and CH8000, Heraeus Clevios) and PSS (Sigma–Aldrich, 18 wt.% in H_2O) thin films (~50 nm-thick),were spun onto the surfaces of the Si wafers. PEDOT:PSS, Dimethyl sulfoxide (DMSO) and poly (4-styrenesulfonic acid) solutions were filtered through a polyvinylidene fluoride membrane (0.22 μm porosity) to remove agglomerations. Thin films were spun coated on the both sides of wafers at 3500–8000 rpm to obtain a similar thickness and subsequently annealed at 130 °C for 10 min in vacuum.

2.2. The solar cell fabrication

180 μm-thick randomly textured n-type Czochralski (CZ)-grown wafers with a resistivity of ~2 Ω·cm were selected. After cleaning and texturization, phosphorus diffusion was carried out in a tube furnace with liquid sources ($POCl_3$) to form the back surface field (BSF). A wet chemical process was performed to remove silicate glass and surface contaminants. A n/n^+ structure was cleaned by a wet chemical process. The front polymer passivation layer (PH1000 + 0.5% DMSO) followed by the front polymer emitter layer (PH1000 + 5%DMSO) were spin coated on the n/n^+ structure. The back Ag pattern was evaporated using a mask. The back polymer passivation layer (AI4083) was coated on the back surface. The solar cell area is approximately 1 cm^2.

2.3. Characterization

After annealing, the samples were transferred immediately into the specific measured environment, such as the 'transparent glass box', or sealed by vacuum (Supplementary Fig. S2). The effective minority carrier lifetime of the double-sided passivated wafer was measured by using the quasi-steady-state (QSS) (when $\tau_{eff} < 100$ μs) and the transient (when $\tau_{eff} > 100$ μs) photoconductance decay techniques on the WCT-120 facility. The chemical composition at the interface was analysed by X-ray photoelectron spectroscopy (XPS) (Thermo escalab 250XI, Al-Ka 1486.6 eV). To clearly probe the interface chemical species, the thin films on Si were repeatedly etched by Ar^+ ions. The absorption spectra were characterized by an optical spectrometer (PerkinElmer, Lambda 950). Ultraviolet photoelectron spectroscopy (UPS) (He I (21.22 eV) emission line) was used to derive the work function and Fermi energy level. The *J-V* characteristics of the solar cells were measured, and the solar cell performance was characterized by

current density-voltage (*J-V*) profiles under the standard test condition (AM1.5, 100 mW/cm^2 and 25 °C).

3. Results and Discussion

3.1. Passivation on the Si surface by PEDOT:PSS thin films

Note that the τ_{eff} of the unpassivated wafer is very low due to high surface recombination, such as only 26.8 μs for the pristine wafer and 130.5 μs for HF-dipped one (Supplementary Fig. S3). It is well known that PEDOT:PSS is sensitive to oxygen and water [36,37]. This fact led us to study the τ_{eff} evolution as the function of testing time in dry and humid air, respectively. As shown in Fig. 1a, the τ_{eff} values of three kinds of PEDOT:PSS-passivated Si wafers show similar tendency in dry air, with a rapid increase in the initial stage and a stable value thereafter. Under exposure to the ambient atmosphere (humid air), τ_{eff} drop instantly and then decay to a low value at a relatively low speed, which indicates that the passivation can be degraded by the adsorption of water from the atmosphere by the PEDOT-PSS layer. A sophisticated analysis concerning this hygroscopic degradation mechanism will be discussed later. Fig. 1b shows the lifetime curves of the maximum value in Fig. 1a, it can be seen that the high quality passivation is confirmed by the high τ_{eff} value of 3.9–6.1 ms, which is more than 10 times the highest value obtained before [30,31]. It is observed that higher PSS ratio leads to higher τ_{eff} (Fig. 1b).

To confirm that the sharp increase of τ_{eff} during the initial stage is associated with O_2 and not to other gases in the air, one sample was first tested under high purity N_2 and then under pure O_2 (Fig. 1c). It can be clearly observed that the initial increase of τ_{eff} is relatively slow under N_2, followed by a rapid increase under O_2, which is similar to the data shown in Fig. 1a for the sample exposed to dry air. Therefore, an oxygen-enhanced mechanism is established for the polymer-passivated Si surface.

To prevent the effect of oxygen and moisture on τ_{eff}, the samples was sealed in a vacuumed transparent plastic bag to obtain an environment with low oxygen and humidity (Supplementary Fig. S2c). Two samples were stored in a "light room" (fluorescent lamp or sunshine) and a dark room respectively once they were not being tested. As shown in Fig. 1d, when the sample is placed in a room with only a fluorescent lamp, τ_{eff} responds slowly as the testing time increases. However, in a sunshine room, τ_{eff} clearly increases from 0.8 to 3.5 ms. For the sample stored in the dark room (in the absence of light, oxygen and moisture), the evolution of τ_{eff} is extremely slow (note that the time scale used is in days), and the value of τ_{eff} is also low. This result indicates that τ_{eff} can be enhanced by irradiation. To verify this point, we carried out a light-soaking test (AM 1.5 G, 1 Sun) for the evolution of τ_{eff} for three sets of PEDOT:PSS-passivated Si wafers, as shown in Fig. 1e. The experiment is operated by means of test cycles, where light soaking is conducted for 1.5 h/test for approximately 20 min in each cycle. It is observed that the τ_{eff} values of the three samples progressively increased as the light soaking time increased until the highest value was reached. In addition, the τ_{eff} values were higher for samples with a higher percentage of PSS (4 ms, 6.2 ms and 6.6 ms corresponding to PEDOT:PSS ratios of 1:2.5, 1:6 and 1:20, respectively).

3.2. Passivation on the Si surface by PSS thin films

We already know from Fig. 1b that the highly effective passivation (i.e., high τ_{eff}) is achieved by the PEDOT:PSS with high percentage of PSS. This necessitates the introduction of a pure PSS thin film as the passivation layer for better passivation. Fig. 2a

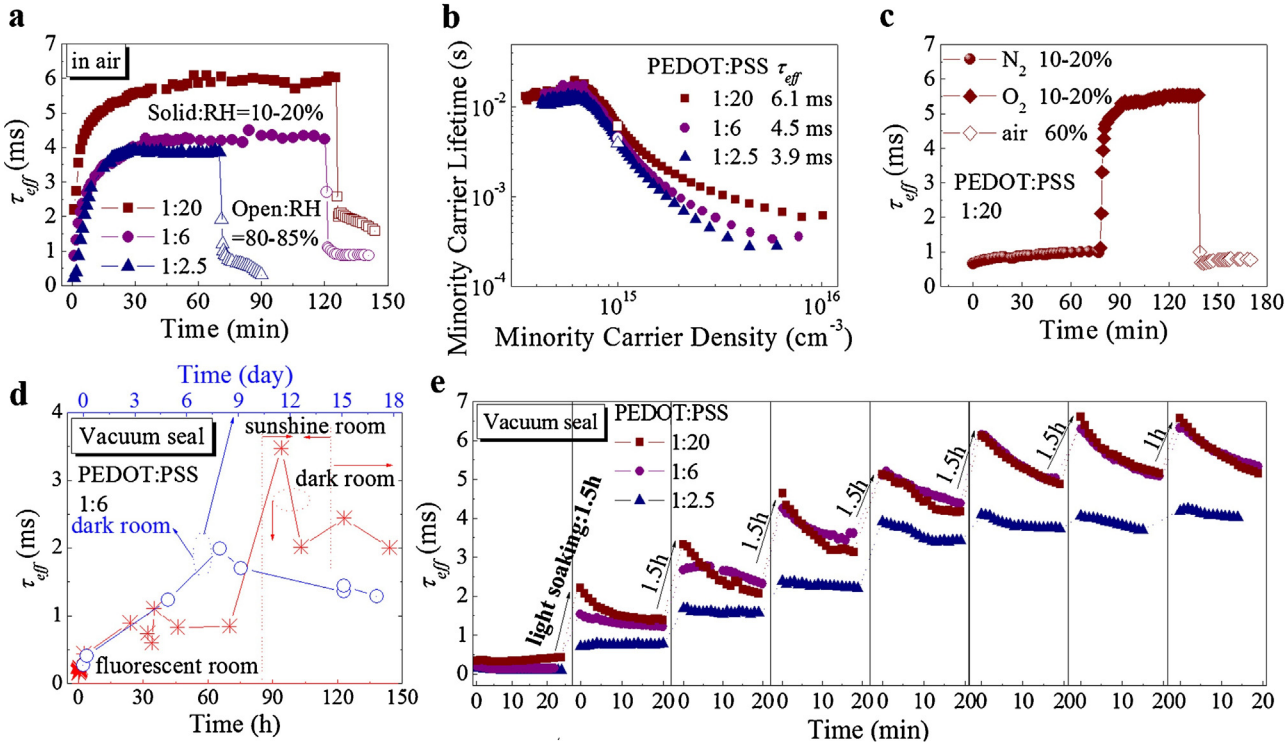

Fig. 1. The lifetime of a PEDOT:PSS thin film-passivated Si surface. The evolution of the lifetime at a minority carrier density of 10^{15} cm^{-3} (τ_{eff}): (a) measured in air with different relative humidity (RH) values, (c) measured first in N_2, then in O_2 and finally in air with a RH > 60%, (d) measured for vacuum-sealed samples stored in a "light room" and a dark room, and (e) measured for vacuum-sealed samples during a light soaking treatment (AM 1.5, 1 Sun). (b) Measured effective minority carrier lifetime as a function of the minority carrier density. RH < 20% was obtained by flowing dry gas in a glass box, and RH > 60% depends on the environment.

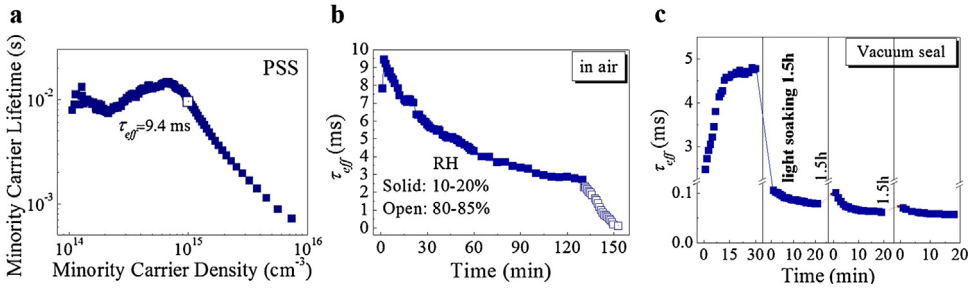

Fig. 2. The lifetime of a PSS thin film-passivated Si surface. (a) Measured effective minority carrier lifetime as a function of the minority carrier density. The evolution of τ_{eff} over the testing time: (b) measured in air with different relative humidity (RH) values, and (c) measured for vacuum-sealed samples during a light soaking treatment (AM 1.5, 1 Sun). PSS thickness: 50 nm.

shows the lifetime curves of the Si wafers passivated by 50 nm-thick PSS thin films alone; it is observed that a τ_{eff} value as high as 9.4 ms (over 6.1 ms by PEDOT:PSS) is obtained. By contrast, if PSS in PEDOT:PSS is decreased, surface passivation should be penalized. In literature it is suggested that DMSO treatment can decrease the percentage of the PSS in PEDOT:PSS [38]. Thus, here DMSO was employed to obtain PEDOT:PSS with less PSS species. We observed that τ_{eff} of the PEDOT:PSS-passivated wafer promptly drops to a very low value (akin to that of the unpassivated wafer) after DMSO treatment (Supplementary Fig. S4). These results sufficiently corroborate the dominant role of the PSS species in PEDOT:PSS for passivation of a Si surface. Further investigation, however, finds that the evolution of τ_{eff} for a Si wafer passivated with only PSS is different from that of a PEDOT:PSS-passivated Si wafer in the following ways: (i) even if in dry air, τ_{eff} does not remain stable, as shown in Fig. 2b; (ii) the value of τ_{eff} clearly reduces after light soaking, as shown in Fig. 2c (Note what τ_{eff} increases at first 30 min before light soaking is affected by the remaining oxygen in the vacuum bag). A thorough explanation of the behaviour above would be elucidated by studying the interface and band line-up of the polymer/Si heterojunction afterward.

3.3. Interface properties and grafting process of PSS molecule on the Si surface

High quality passivation denotes low interface defects, which is closely linked to the polymer/Si interface properties. The analysis was performed using XPS. Taking into account that the wafer was coated by 50 nm-think polymer layer that transcends the probe range (5–10 nm) of XPS [39], we removed it by Ar^+ etching until a possible interface was identified. The interface identification can be estimated by the analysis of the atomic percentage of Si and S (Supplementary Fig. S5). Fig. 3a shows the Si 2p XPS spectra of PEDOT:PSS (1:20)-passivated Si wafers, including the samples with and without light soaking treatment. Sub-oxide states of Si (SiO_x, $x < 2$), corresponding to several valence states from Si^{1+} to Si^{4+}, are detected aside from the Si species (Si^0) located at 99.3–99.8 eV [40], which indicates that the Si surface is progressively oxidized. This result is consistent with the study by S. Jäckle, et al. [38] and unveils the nature of passivation by these polymer thin films, i.e. the occurrence of oxidation at polymer/Si interface. It is well known that the oxide signal was not detected for the freshly HF-treated wafer [41]. It is also clearly observed that the peak intensities of the sub-oxides for the sample with light soaking are stronger than those of the one without light soaking. This result indicates that oxidation is promoted by the light soaking treatment, which agrees with the τ_{eff} trends. Additionally, as shown in Fig. 3b, a stronger oxidation signal is displayed in the Si 2p XPS spectra of the Si wafer well-passivated by PSS alone and a little of the oxide signal is found in Si 2p XPS spectra of the sample with failure passivation exposed in the ambient atmosphere for 24 h, which further indicates that high-quality passivation is dominated by PSS oxidization to Si surface.

To determine the origin of oxidation at the PSS/Si interface, we performed the structure optimization and the electron localization function (ELF) analysis for the feasible grafting process using first-principles total-energy calculations (Computational Methods can be found in the supporting information). As shown in Fig. 4, two representative adsorption structures were obtained from various adsorption geometries of PSS monomer molecule (Supplementary Fig. S6a) adsorption on the H-terminated Si (001) surface with dangling bonds (Supplementary Fig. S6b). The grafting process

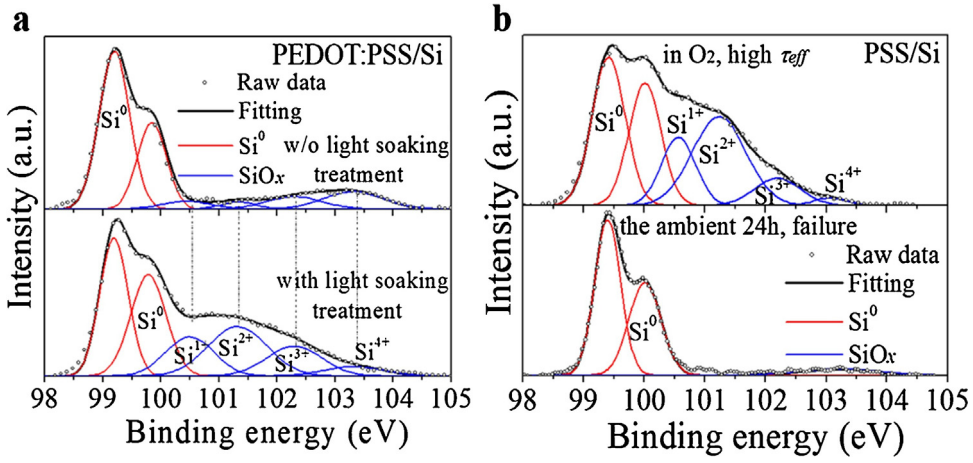

Fig. 3. Interface characterization. (a) Si 2p XPS spectra of PEDOT:PSS (1:20)-passivated wafers with and without the light soaking treatment and (b) PSS-passivated wafers with the measurement performed in O_2 to obtain high τ_{eff} and exposed to the ambient environment for 24 h.

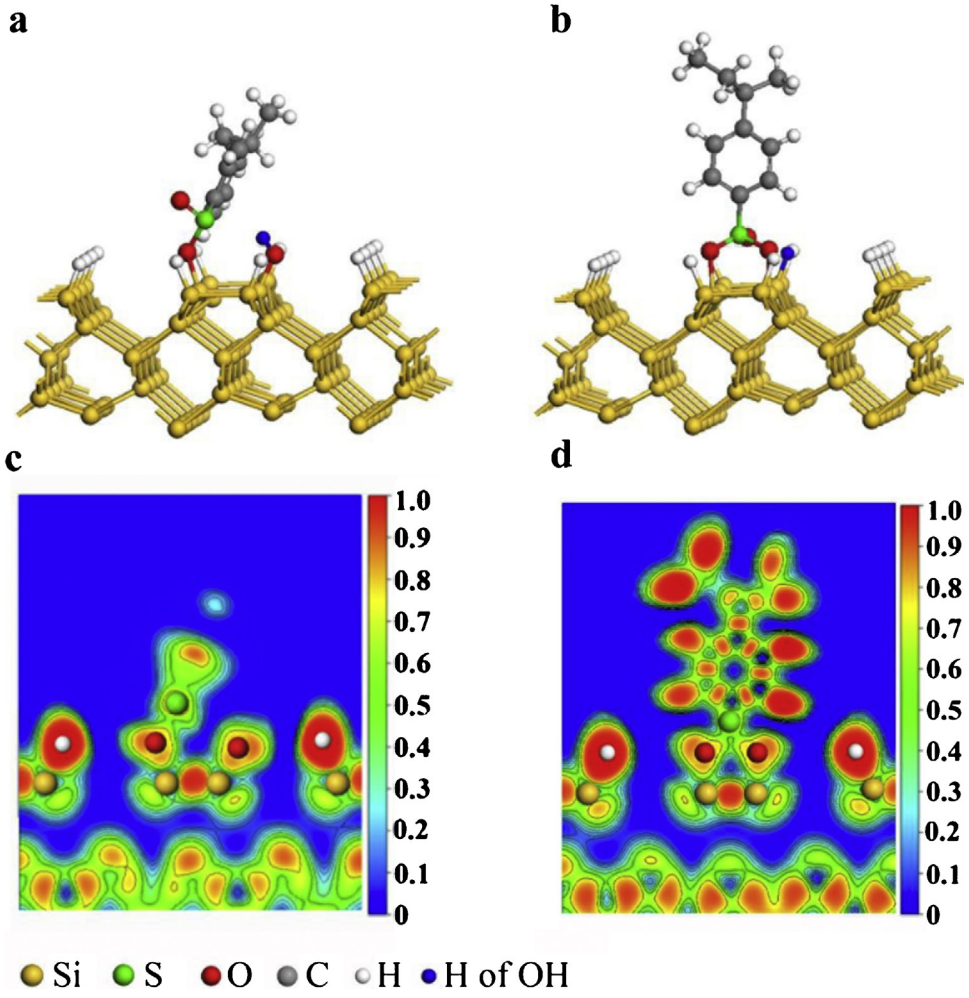

Fig. 4. Grafting mechanism. (a) and (b) Two stable structures for the PSS molecule grafted on the H-terminated Si surface. (c) and (d) The corresponding ELFs for the two structures.

comprises two aspects: (i) the formation of Si—O—H after the breakaway of hydroxyl from PSS and Si—O—R when one of the O groups in the surplus O-containing constituent (denoted using 'R') in PSS is grafted on the activated Si surface, and the removal of the H-atom at the Si surface, as observed in Fig. 4a and c; (ii) the bonding of the H atom of hydroxyl in PSS with the Si atom after it is removed from PSS. Meanwhile, the two O atoms of PSS bond with Si to form Si—O—R, as shown in Fig. 4b and d. It is well known that ELF can generally reflect the bonding information, i.e., the perfect localization (covalent bonding), the electron-gas-like pair probability (metallic bonding) and the ionic bonding (precursor to metal bonding) correspond to ELF values of 1, 0.5 and 0, respectively [42]. Here, Si and O form a metallic bond between covalent and ionic one. The corresponding adsorption energies of the two structures as shown in Fig. 4a and b are −2.73 eV and −1.86 eV, respectively, which indicates that these configurations are feasible. Therefore, we attempt to provide a grafting scheme that corresponds to the following equation:

$$\equiv \mathrm{Si}\cdot + \ \mathrm{PSS} \rightarrow \mathrm{Si} - \mathrm{O} - \mathrm{R}' \qquad (1)$$

where R′ denotes three constituents, including '−H' from the sulfonic acid group and the two remaining constituents in the PSS molecule, as shown in Fig. 4a and b. These species may coexist in the experiments according to the values of the adsorption energies.

3.4. Electrochemical behaviour of passivation

It is observed that τ_{eff} increases after light soaking and decreases in the light-off cycle testing (Fig. 1e), showing a reversible behaviour. The light soaking is associated with the charge injection. Here, an external field is applied to execute the charge injection. The sputtered ITO thin film and low-resistivity Si (for better conductivity) are introduced as electrodes, and the geometry of the sample is shown in the inset of Fig. 5. The initial τ_{eff} of the PSS/n-Si/PSS sample is 283 μs, whereas the τ_{eff} of the ITO/PSS/n-Si/PSS/ITO sample decreases to 31 μs after ITO deposition. The observed degradation is partially due to the ion bombardment and partial irradiation by the sputtered plasma (Supplementary Fig. S7), which results in a situation where τ_{eff} cannot be fully restored likely due to the microstructural irreversibility of the material. The evolution of τ_{eff} is shown in Fig. 5; a low value is observed after ITO deposition, then the τ_{eff} of the sample progressively increases as the applied voltage increases from +1.1 to +1.5 V. This indicates that the applied potential can also lead to the oxidation of the Si surface, which is in accordance with the light-induced passivation enhancement. After poling by applying a larger negative voltage of −3.5 V, τ_{eff} drops instantly from 138 μs to 34 μs, which indicates that the deoxidation may happen. During repetitive oxidation cycles at +1.5 V and deoxidation cycles at

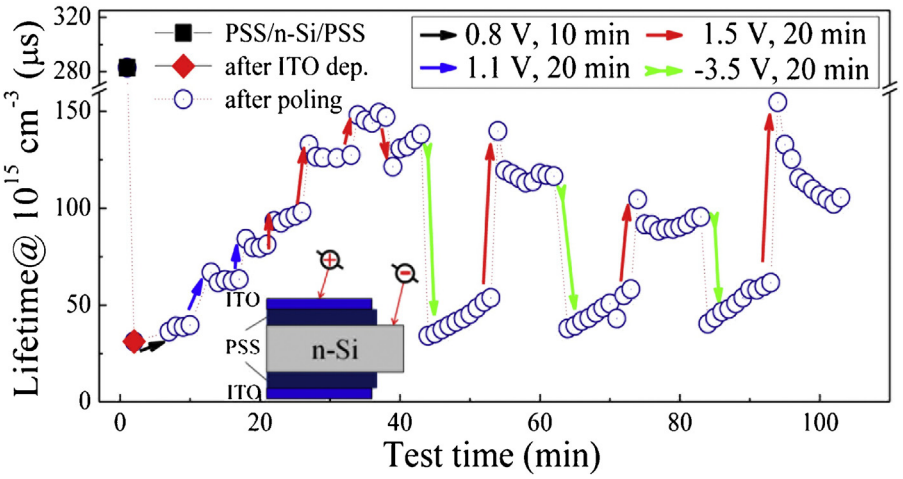

Fig. 5. Electrochemically switchable behaviour of τ_{eff}. The inset is a test structure. A 200 μm-thick n-type (100)-oriented CZ-Si wafer (1–5 Ω cm) was selected to achieve the electric measurement. The poling direction is termed to be positive if a positive bias voltage is applied to the top ITO electrode.

−3.5 V, a switchable electrochemical behaviour of τ_{eff} is presented. This result further confirms the origin of electrochemical passivation for the PSS-passivated Si surface.

Therefore, the reaction in Eq. (1) is a redox reaction, which can be described as the following:

$$\equiv \mathrm{Si}\cdot + \mathrm{PSS} \underset{e^-}{\overset{h^+}{\rightleftharpoons}} \mathrm{Si} - \mathrm{O} - \mathrm{R}' \qquad (2)$$

where holes and electrons are denoted by h^+ and e^-, respectively. Because the redox reaction is a reversible reaction, when the Si surface acts as an electron donor, the amount of Si dangling bonds increases, and the forward reaction (from the left side to the right ride in Eq. (2)) is favoured while the reverse reaction is suppressed. By contrast, when the Si surface acts as an electron acceptor, the reverse reaction is favoured and the forward reaction is suppressed.

3.5. Charge transport

It can be concluded that the passivation effect of the PSS thin film originates from the oxidation on the Si surface to reduce the surface dangling bonds, and light soaking can increase this oxidation. Now the following questions arise: (i) Why and how does light soaking improve oxidation? (ii) Why does τ_{eff} increase for the sample passivated by PEDOT:PSS but decrease for the sample passivated by PSS alone after light soaking? (iii) Why does τ_{eff} remain stable in dry air for the former but not for the latter? The

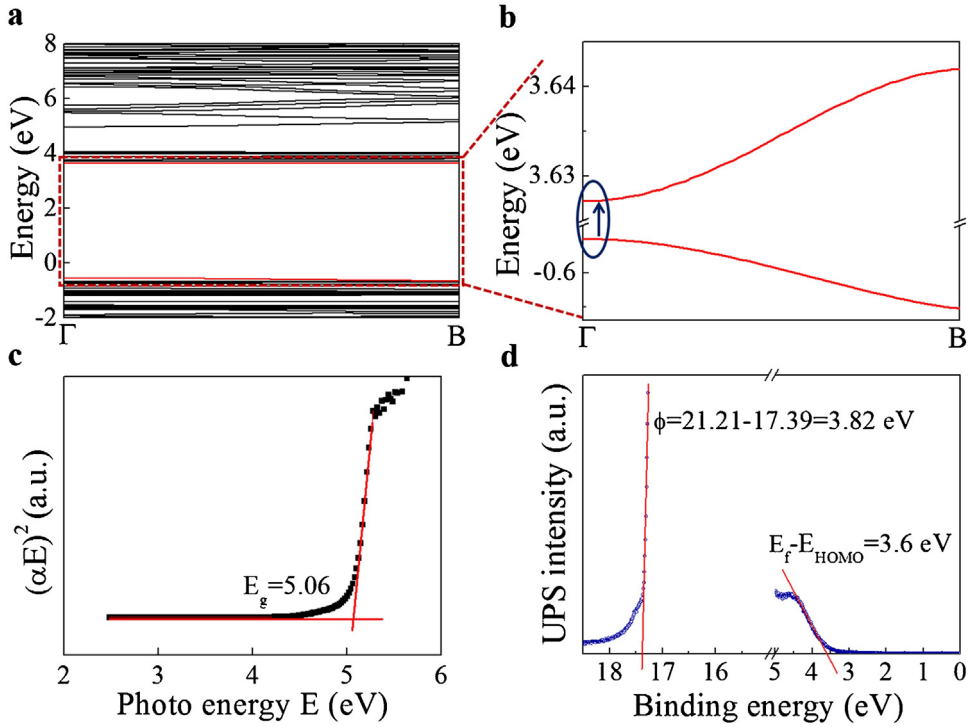

Fig. 6. The energy band information of PSS thin films. (a) The calculated energy band structure of PSS. (b) The larger image for detail position in (a). (c) $(\alpha E)^2$ vs E to obtain the optical band gap of PSS thin film. (d) UPS cut off spectra of PSS thin film.

answers to these questions are related to charge transfer at the interface.

To analyse the interfacial charge transport behaviour, the band line-up of heterojunction is first studied. Numerous publications have investigated the band information of Si and PEDOT:PSS materials, such as the optical band gap E_g, work function Φ, and the position of the Fermi energy level ($E_f - E_v$) [43,44]. However, little is known about the nature of the PSS thin film material let alone its band information. In this work, we first employed the first-principles calculation to determine that PSS is a direct gap material (Fig. 6a and b) and then measured the UV–vis absorption spectra of the PSS thin film on a glass substrate to validate that its optical band gap is 5.06 eV by the direct optical transitions illustrated by the $(\alpha E)^2$ versus E plots (Fig. 6c). Finally, UPS was used to derive values of $\Phi = 3.83$ eV and $E_f - E_v = 3.6$ eV (Fig. 6d). The energy-band diagrams of the materials are illustrated in Fig. 7a. Unexpectedly, PEDOT:PSS is a well-known p-type material [21,24,27], whereas the PSS thin film is found to be an n-type material (Fig. 7a shows that E_f is near the conduction band). According to the data in Fig. 7a, the band line-ups of PEDOT:PSS/n-c-Si/PEDOT:PSS and PSS/n-c-Si/PSS can be determined, as shown in Fig. 7b and c, and the charge transfer information are also sketched in the figures.

In Fig. 7b, due to work function (Φ) of PEDOT:PSS (denoted by Φ_{PD}) > Φ_{Si}, the band of PEDOT:PSS bends down and the Si band bends up at the interface, which builds an internal field (E_{in}) with its direction from Si to PEDOT:PSS. Upon light soaking, photo-excited electron-hole pairs are created and separated by E_{in}. At this moment, holes are transferred from the Si bulk to the surface, and electrons are transferred from the Si surface into the bulk. Therefore, the Si surface plays the role of an electron donor and a hole acceptor, which results in an increase of the reactant ($\equiv Si^{\bullet}$) in Eq. (2). This means that the forward reaction in Eq. (2) is favoured, which results in an increase of the Si surface oxidation and an extreme improvement of passivation. Fig. 7c reveals the band line-ups of PSS/n-c-Si/PSS. Contrary to PEDOT:PSS, $\Phi_{PSS} < \Phi_{Si}$, so the PSS band bends up and the Si band bends down, which results in the build-up of E_{in} with its direction from PSS to Si. Upon light soaking, electrons are transferred from the Si bulk to the surface, and the Si surface behaves as an electron acceptor, which leads to a decrease of the reactant in Eq. (2). In this case, the reverse reaction in Eq. (2) is favoured, which results in a reduced surface oxidation and passivation. The stability of τ_{eff} in dry air is also determined by the direction of E_{in}. If the E_{in} direction is beneficial to electron transfer from the Si surface to the bulk, E_{in} will hamper electron injection into the Si surface and τ_{eff} will remain stable. Otherwise, E_{in} cannot impede electron injection into the Si surface, and the amount of the reactant is gradually decreased, which means that τ_{eff} does not remain stable.

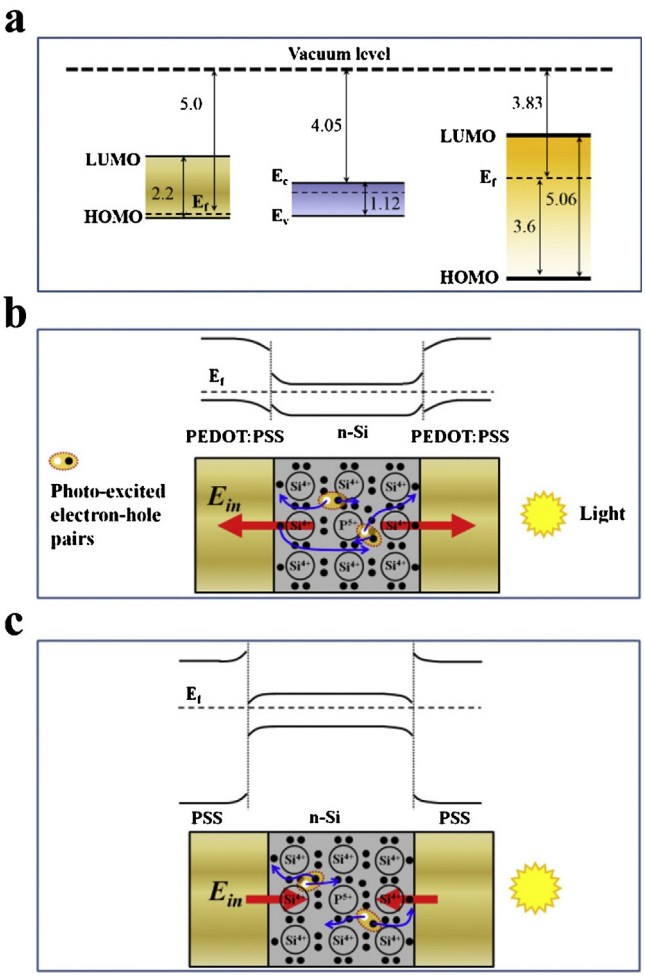

Fig. 7. Band line-up and the charge transfer information. (a) Schematic energy diagrams of PEDOT:PSS (left, PH1000, Heraeus Clevios), n-Si (middle) and PSS (right, Sigma–Aldrich, 18 wt.% in H_2O). Band line-up and the sketch of the charge transfer information of (b) PEDOT:PSS/n-Si/PEDOT:PSS and (c) PSS/n-Si/PSS heterojunction.

We term the difference of Φ and E_{in} between the PSS and Si as $\Delta\Phi_1$ and E_1, respectively. Similarly, the difference between the Φ and E_{in} of PEDOT:PSS and PSS are denoted as $\Delta\Phi_2$ and E_2, respectively. Simply put, $\Delta\Phi_2$ (1.17 eV) > $\Delta\Phi_1$ (0.22 eV) and therefore, $E_2 > E_1$. Based on this result, a heterojunction stack PEDOT:PSS/PSS/n-c-Si/PSS/PEDOT:PSS is fabricated, and its band line-up is observed in Supplementary Fig. S8a. Because $E_2 > E_1$, the total direction of the field E_{in} in the stack structure can be internally reversed. According to the analysis above, the evolution of τ_{eff} for this heterojunction stack should follow the same trend as PEDOT:PSS/n-c-Si/PEDOT:PSS, i.e., it should be stable in dry air and enhanced by light soaking. Our data confirm these points (Supplementary Fig. S8b and c).

It is mentioned that whenever PEDOT:PSS or PSS exhibits a passivation behaviour, passivation is enhanced in an oxygen atmosphere and then degraded in a humid environment. Based on the understanding of the passivation origin (vide supra), this behaviour is explained as follows. On the one hand, it has been reported that oxygen can diffuse through PEDOT:PSS thin films due to the gas permeability of this material [39]. In the PSS/Si heterointerface, the penetrating oxygen can oxidize the Si surface and transform it to an electron donor. This will accelerate the forward reaction in Eq. (2) and lead to further oxidation of the Si surface by PSS, which improves passivation. This process is sketched in Supplementary Fig. S9. On the other hand, the PSS would absorb water from the ambient atmosphere and become an electron donor via [45]:

$$2\mathrm{PSS(Si)} + \mathrm{H_2O} \rightarrow 2\mathrm{PSSH} + \frac{1}{2}\mathrm{O_2} + 2\mathrm{e^-} \quad (3)$$

Clearly, the process in Eq. (3) will contribute electrons to the Si surface, which favours the reverse reaction in Eq. (2) and results in the degradation of passivation.

3.6. Implications and applications for solar cells

Based on the understanding of the origin of polymer passivation on the Si surface, further investigation of the solar cells was performed to examine the application to real devices. We have determined that PEDOT:PSS and PSS alone both have an excellent passivation effect, but they behave differently with light. The former exhibits light-induced enhancement, but the latter shows light-induced degradation. This means that PSS is not suitable for

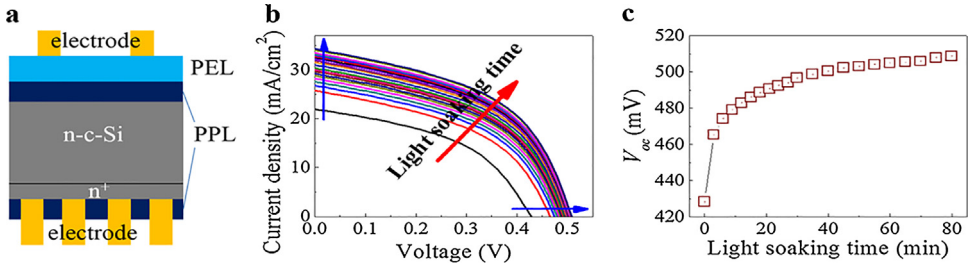

Fig. 8. Solar cells. (a) The geometry of a polymer passivated both-sides Si heterojunction solar cell. In this device geometry, PH1000 with the addition of 0.5% DMSO, PH1000 with the addition of 5% DMSO and Al4083 were used as the front PPL, the rear PPL and PEL. Ag thin films were employed as the electrode materials. (b) J–V curves of the solar cell under light soaking. (c) The plot of V_{oc} as function of light soaking time.

the passivation of n-type Si surfaces. In the experiments above, n-type Si substrates was selected to determine the degree of passivation. For p-type Si, it is easy to infer that light-induced passivation degradation will be more severe since the difference between the work function of p-type Si and PSS is greater than that between n-type Si and PSS (Supplementary Fig. 10a). Therefore, the PSS thin film here is plausibly only useful for measuring the quality of the Si material and not for solar cell devices. By considering the origin of passivation, the light-induced passivation degradation of the PSS-passivated Si surface originates from the injection of electrons into the Si surface. If this injection is hampered, the problem of degradation will be alleviated. Thus, PSS is deemed to be more suitable as a p-side surface in conventional p-n junction Si solar cells because the barrier in the pn junction can inhibit the injection of electrons and promote the injection of holes. The τ_{eff} of PSS/p/n/n^+/PEDOT:PSS was examined by a light soaking treatment, as shown in Supplementary Fig. 10b, a small light-induced passivation enhancement was observed rather than degradation.

PEDOT:PSS and p-type Si have similar work functions, thus, a poor light-induced passivation enhancement is observed (Supplementary Fig. 10c). Therefore, more consideration will be given to the application of PEDOT:PSS in n-type Si solar cells. In this study, a new concept, a polymer-passivated both-sides Si heterojunction solar cell, is developed to evaluate our findings, and the geometry of the device is shown in Fig. 8a. In this device, a polymer passivation layer (PPL), followed by a polymer emitter layer (PEL), is coated on a randomly textured n-type CZ c-Si wafer to form a p-n heterojunction. On the other side of the c-Si wafer, the diffused n^+ back surface field (BSF), followed by a patterned PPL based on the local passivation strategy, and the patterned metallization are fabricated. By introducing the PPL on both sides of the Si substrate, the defects on the c-Si surface can be effectively passivated. The PEL also functions as an antireflection coating due to the refractive index of PEDOT:PSS [46]. Either PEDOT:PSS or PSS films can be selected as the PPL, and PH1000 with the addition of 5% DMSO is used as the PEL. *J-V* curves and photovoltaic parameters of the solar cell are displayed in Fig. 8b and Table 1. It is clearly observed that all parameters of this device, including the J_{sc}, V_{oc} and FF, increase dramatically as the light soaking time increases. The light-induced V_{oc} improvement is clearly a result of the light-induced passivation enhancement (Figs. 8c and 1e). It has been reported that the valance band of PEDOT is increased by 0.4 eV when PEDOT is oxidized by the injection of holes [47,48]. This effect could result in a reduction of valance band offset in the PEDOT:PSS/Si heterojunction solar cell and the subsequent improvement of J_{sc} and FF. Another partial reason for the increase of J_{sc} is light-induced temperature increase (from 25 to 40 °C).

Table 1
PV performance of the solar cells.

Light soaking time (min)	V_{oc} (mV)	J_{sc} (mA/cm^2)	FF (%)	PCE (%)
0	428.2	21.95	45.9	4.32
3	465.2	25.74	45.9	5.50
15	481.1	28.80	47.3	6.63
30	496.7	30.97	48	7.39
60	504.8	32.97	48.7	8.10
70	505.9	33.46	48.7	8.25
75	507.8	34.02	49.0	8.46
80	508.6	34.30	48.9	8.54

4. Conclusions

In summary, we show a high-quality passivation of Si surfaces by polymer thin films: PSS and/or PEDOT:PSS with the appropriate percentage of PSS species. A millisecond level lifetime has been achieved by a PSS thin film. Henceforth, PSS is not only used as a dispersant for the solubilization of PEDOT but also as a novel functional thin film material to suppress Si recombination. The origin of polymer passivation is demonstrated to be an electrochemical oxidation/deoxidation process at the PSS/Si interface. This process can be controlled via electron transfer at the Si surface. The electron transfer can be tuned by modifying the following: (i) the oxygen atmosphere, (ii) the internal field combining with light soaking, (iii) the external field by the applied bias, and (iv) the water in the atmosphere. Passivation can be enhanced by (i), (ii) and (iii) and degraded by (ii), (iii) and (iv). The passivation scheme and mechanism are examined by applying them to real devices. A new solar cell concept, a polymer passivated both-sides Si heterojunction solar cell is developed. Following with the lifetime evolution, a light-induced enhancement of the PV performance is observed.

Acknowledgements

This work is supported by NSF of Hebei Province (E2015201203), Advanced Talents Program of Hebei Province (GCC2014013), Top Young Outstanding Innovative Talents Program of Hebei Province (BJ2014009), The Midwest universities comprehensive strength promotion project (1060001010314), NSF of Hebei Province (F2015201189), “100 Talents Program of Hebei Province” (E2014100008) and ISTCP of China (2015DFE62900).

Appendix A. Supplementary data

Supplementary data associated with this article can be found, in the online version, at http://dx.doi.org/10.1016/j.electacta.2017.07.071.

References

[1] J. Oh, H.C. Yuan, H.M. Branz, An 18.2%-efficient black-silicon solar cell achieved through control of carrier recombination in nanostructures, Nat. Nanotechnol. 7 (2012) 743–748.

[2] B. Hoex, J. Schmidt, P. Pohl, M.C.M. van de Sanden, W.M.M. Kessels, Silicon surface passivation by atomic layer deposited Al_2O_3, J. Appl. Phys. 104 (2008) 044903.
[3] T. Mueller, S. Schwertheim, M. Scherff, W.R. Fahrner, High quality passivation for heterojunction solar cells by hydrogenated amorphous silicon suboxide films, Appl. Phys. Lett. 92 (2008) 033504.
[4] B. Chhabra, S. Bowden, R.L. Opila, C.B. Honsberg, High effective minority carrier lifetime on silicon substrates using quinhydrone-methanol passivation, Appl. Phys. Lett. 96 (2010) 063502.
[5] A.W. Stephens, M.A. Green, Novel method for minoritycarrier mobility measurement using photoconductance decay with chemically passivated and plasma damaged surfaces, J. Appl. Phys. 80 (1996) 3897.
[6] M. Lu, U. Das, S. Bowden, S. Hegedus, R. Birkmire, Optimization of interdigitated back contact silicon heterojunction solar cells, tailoring hetero-interface band structures while maintaining surface passivation, Prog. Photovolt. Res. Appl. 19 (2011) 326–338.
[7] S. Zhao, Q. Qiao, S. Zhang, J. Ji, Z. Shi, G. Li, Rear passivation of commercial multi-crystalline PERC solar cell by PECVD Al_2O_3, Appl. Surf. Sci. 290 (2014) 66–70.
[8] H. Savin, P. Repo, G. von Gastrow, P. Ortega, E. Calle, M. Garin, R. Alcubilla, Black silicon solar cells with interdigitated back-contacts achieve 22.1% efficiency, Nat. Nanotechnol. 10 (2015) 624–628.
[9] B. Demaurex, W.S. De, A. Descoeudres, H.Z. Charles, C. Ballif, Damage at hydrogenated amorphous/crystalline silicon interfaces by indium tin oxide overlayer sputtering, Appl. Phys. Lett. 101 (2012) 171604.
[10] H.P. Zhou, D.Y. Wei, S. Xu, S.Q. Xiao, L.X. Xu, Crystalline silicon surface passivation by intrinsic silicon thin films deposited by low-frequency inductively coupled plasma, J. Appl. Phys. 112 (2012) 013708.
[11] Z.R. Chowdhury, K. Cho, N.P. Kherani, High-quality surface passivation of silicon using native oxide and silicon nitride layers, Appl. Phys. Lett. 101 (2012) 021601.
[12] M.J. Kerr, C. Andres, Very low bulk and surface recombination in oxidized silicon wafers, Semicond. Sci. Technol. 17 (2002) 35–38.
[13] D.S. Wolf, M. Kondo, Abruptness of a-Si:H/c-Si interface revealed by carrier lifetime measurements, Appl. Phys. Lett. 90 (2007) 042111.
[14] I. Jozwik, P. Papet, A. Kaminski, E. Fourmond, F. Calmon, M. Lemiti, Interdigitated back contact solar cells with SiO_2 and SiN back surface passivation, Journal of Non-Crystalline Solids 354 (2008) 4341–4344.
[15] D. Macdonald, R.A. Sinton, A.S. Cuevas, On the use of a bias-light correction for trapping effects in photoconductance-based lifetime measurements of silicon, J. Appl. Phys. 89 (2001) 2772.
[16] B. Liao, R. Stangl, T. Mueller, F. Lin, C.S. Bhatia, B. Hoex, The effect of light soaking on crystalline silicon surface passivation by atomic layer deposited Al_2O_3, J. Appl. Phys. 113 (2013) 024509.
[17] A. Descoeudres, L. Barraud, Stefaan De Wolf, B. Strahm, D. Lachenal, C. Guérin, Z.C. Holman, F. Zicarelli, B. Demaurex, J. Seif, J. Holovsky, C. Ballif, Improved amorphous/crystalline silicon interface passivation by hydrogen plasma treatment, Appl. Phys. Lett. 99 (123506) (2011).
[18] P.P. Altermatt, K.R.T. McIntosh, A roadmap for PERC cell efficiency towards 22% focused on technology-related constraints, Energy Procedia 55 (2014) 17–21.
[19] K. Matsuyama, A. Yano, S. Tohoda, Y. Nakamura, T. Nishiwaki, K. Fujita, M. Taguchi, E. Maruyama, Development of HIT® solar cell for exceeding 25% conversion efficiency, Grand Renewable Energy (2014) Abstracts, 27 July–1 August 2014.
[20] Kunta Yoshikawa, Hayato Kawasaki, Wataru Yoshida, Toru Irie, Katsunori Konishi, Kunihiro Nakano, Toshihiko Uto, Daisuke Adachi, Masanori Kanematsu, Hisashi Uzu, Kenji Yamamoto, Silicon heterojunction solar cell with interdigitated back contacts for a photoconversion efficiency over 26%, Nature Energy 2 (2017) 17032.
[21] J.P. Thomas, K.T. Leung, Defect-Minimized PEDOT:PSS/Planar-Si Solar Cell with Very High Efficiency, Adv. Funct. Mater. 24 (2014) 4978–4985.
[22] D. McGillivray, J.P. Thomas, M. Abdellah, N.F. Heinig, K.T. Leung, Performance Enhancement by Secondary Doping in PEDOT:PSS/Planar-Si Hybrid Solar Cells, ACS Appl. Mater. Interfaces 8 (2016) 34303–34308.
[23] J. Kim, et al., 10.5% efficient polymer and amorphous silicon hybrid tandem photovoltaic cell, Nat. Commun. 6 (2015) 6391.
[24] D. Zielke, A. Pazidis, F. Werner, J. Schmidt, Organic-silicon heterojunction solar cells on n-type silicon wafers: The BackPEDOT concept, Sol. Energ. Mat. Sol. C 131 (2014) 110–116.
[25] M. Junghanns, et al., PEDOT:PSS emitters on multicrystalline silicon thin-film absorbers for hybrid solar cells, Appl. Phy. Lett. 106 (2015) 083904.
[26] W.-R. Wei, et al., Above-11%-efficiency organic-inorganic hybrid solar cells with omnidirectional harvesting characteristics by employing hierarchical photon-trapping structures, Nano Lett. 13 (2013) 3658–3663.
[27] J. Sheng, et al., Improvement of the SiOx passivation layer for high-efficiency Si/PEDOT:PSS heterojunction solar cells, ACS Appl. Mater. Interfaces 6 (2014) 16027–16034.
[28] E. Yablonovitch, D.L. Allara, C.C. Chang, T. Gmitter, T.B. Bright, Unusually Low Surface-Recombination Velocity on Silicon and Germanium Surfaces, Phys. Rev. Lett. 57 (1986) 249.
[29] H. M'saad, J. Michel, J. Lappe, L.C. Kimerling, Electronic Passivation of Silicon Surfaces by Halogens, J. Electron. Mater. 23 (1994) 487.
[30] M. Yameen, S.K. Srivastava, P. Singh, K. Turan, P. Prathap, C.M.S. Vandana Rauthan, P.K. Singh, Low temperature fabrication of PEDOT:PSS/micro-textured silicon-based heterojunction solar cells, J. Mater. Sci. 50 (2015) 8046–8056.
[31] T. Subramani, H.J. Syu, C.T. Liu, C.C. Hsueh, S.T. Yang, C.F. Lin, Low-Pressure-Assisted Coating Method To Improve Interface between PEDOT:PSS and Silicon Nanotips for High-Efficiency Organic/Inorganic Hybrid Solar Cells via Solution Process, ACS Appl. Mater. Interfaces 8 (2016) 2406–2415.
[32] L. Zhao, et al., The Effects of Improved Photoelectric Properties of PEDOT:PSS by Two-Step Treatments on the Performance of Polymer Solar Cells Based on PTB7-Th:PC71BM, ACS Appl. Mater. Interfaces 8 (2015) 547–552.
[33] Y. Zhang, et al., High efficiency hybrid PEDOT:PSS/nanostructured silicon Schottky junction solar cells by doping-free rear contact, Energy Environ Sci. 8 (2015) 297–302.
[34] I. Lee, G.W. Kim, M. Yang, T.S. Kim, Simultaneously Enhancing the Cohesion and Electrical Conductivity of PEDOT:PSS Conductive Polymer Films using DMSO Additives, ACS Appl. Mater. Interfaces 8 (2016) 302–310.
[35] J.G. Chen, H.Y. Wei, K.C. Ho, Using modified poly(3, 4-ethylene dioxythiophene): Poly(styrene sulfonate) film as a counter electrode in dye-sensitized solar cells, Sol. Energ. Mat. Sol. C 91 (2007) 1472–1477.
[36] H.S. Kang, H.S. Kang, J.K. Lee, J.W. Lee, J. Joo, J.M. Ko, M.S. Kim, J.Y. Lee, Humidity-dependent characteristics of thin film poly(34-ethylenedioxythiophene) field-effect transistor, Synth. Met. 155 (2005) 176–179.
[37] K. Kawano, R. Pacios, D. Poplavskyy, J. Nelson, D.D.C. Bradley, J.R. Durrant, Degradation of organic solar cells due to air exposure, Sol. Energy Mat. Sol. C 90 (2006) 3520–3530.
[38] S. Jäckle, M. Liebhaber, J. Niederhausen, M. Büchele, R. Fe'lix, R.G. Wilks, M. Bär, K. Lips, S. Christiansen, Unveiling the Hybrid n-Si/PEDOT:PSS Interface, ACS Appl. Mater. Interfaces 8 (2016) 8841.
[39] K. Norrman, M.V. Madsenet, S.A. Gevorgyan, F.C. Krebs, Degradation Patterns in Water and Oxygen of an Inverted Polymer Solar Cell, J. Am. Chem. Soc. 132 (2010) 16883–16892.
[40] C. Gondek, M. Lippold, I. Röver, K. Bohmhammel, E. Kroke, Etching Silicon with HF-H_2O_2-Based Mixtures: Reactivity Studies and Surface Investigations, J. Phys. Chem. C 118 (2014) 2044–2051.
[41] D. Graf, M. Grundner, R. Schulz, Oxidation of HF-treated Si wafer surfaces in air, J. Appl. Phys. 68 (1990) 5155.
[42] A.D. Becke, K.E. Edgecombe, A simple measure of electron localization in atomic and molecular systems, J. Phy. Chem. C 92 (1990) 5397–5403.
[43] C. Brabec, V. Dyakonov, U. Scherf, Organic Photovoltaics 213 (2009).
[44] S. Jackle, M. Mattiza, M. Liebhaber, G. Bronstrup, M. Rommel, K. Lips, S. Christiansen, Junction formation and current transport mechanisms in hybrid n-Si/PEDOT:PSS solar cells, Sci. Rep. 5 (2015) 13008.
[45] S. Möller, S.R. Forrest, C. Perlov, W. Jackson, C. Taussig, Electrochromic conductive polymer fuses for hybrid organic/inorganic semiconductor memories, J. Appl. Phys. 94 (2003) 7811–7819.
[46] C. Brabec, V. Dyakonov, U. Scherf (Eds.), Organic Photovoltaics: Materials, Device Physics, and Manufacturing Technologies, Wiley-VCH, Weinheim, 2008.
[47] S. Møller, C. Perlov, W. Jackson, C. Taussig, S.R. Forres, A polymer/semiconductor write-once read-many-times memory, Nature 426 (2003) 166–169.
[48] E. Yablonovitch, T. Gmitter, Auger recombination in silicon at low carrier densities, Appl. Phys. Lett. 49 (1986) 587.